1. Supplemental Figures

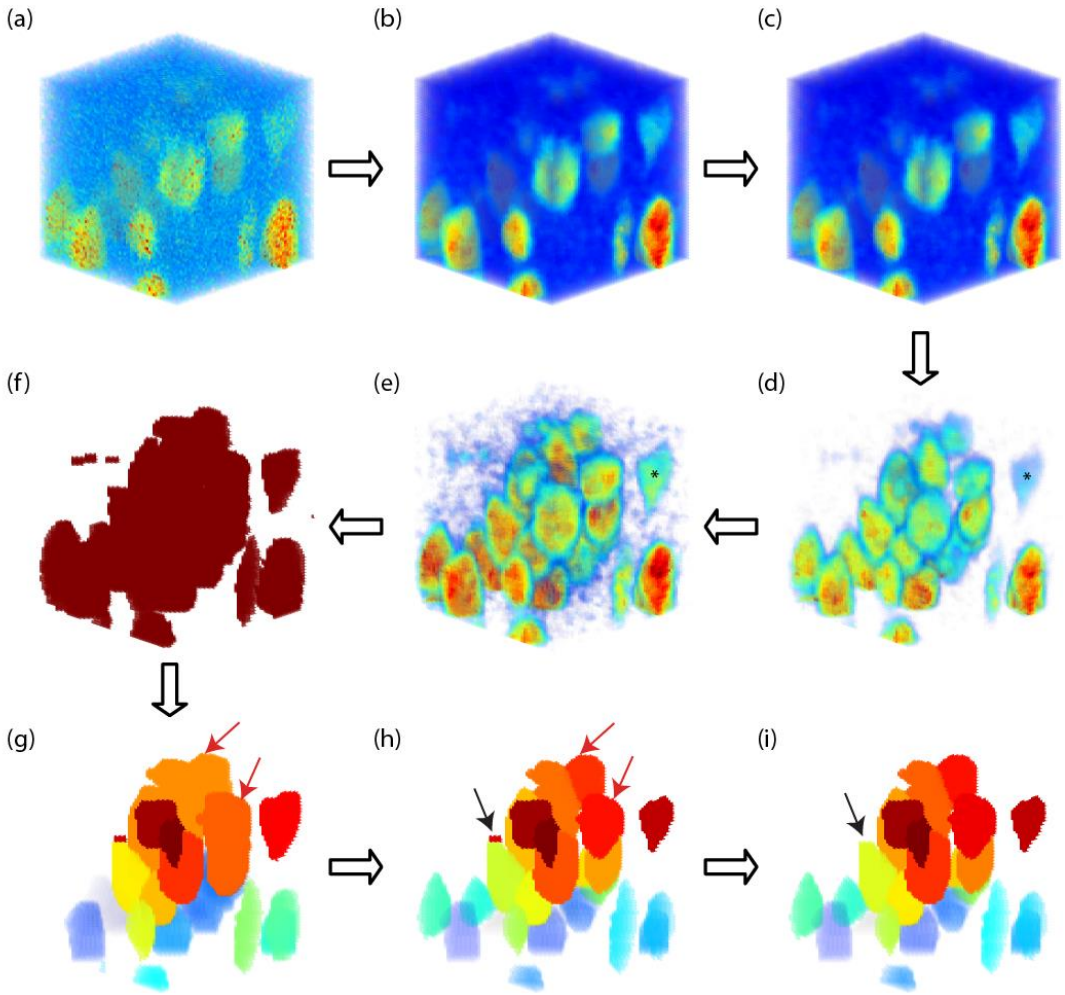

Supplemental Figure 1.

Automatic cell counting for soma-staining channels. The example is an anti-NeuN+ staining volume. (a) Original 3D image stack obtained from Z-scan confocal imaging. (b) Median filtering with a 3-by-3-by-3 pixel neighborhood to reduce local intensity variation in the image. (c) Vignetting correction using single-image based method. (d) Background subtraction to reduce the background intensity level. (e) Contrast-limited adaptive histogram equalization (CLAHE) to enhance local contrast. Notice the contrast enhancement effect on the weakly stained cell marked with * in (d) and (e). (f) Black-and-white (B&W) transform to separate foreground objects from the background. (g) Marker-base watershed segmentation on the BW image. Identified objects are labelled with different colors. Notice the cell clusters pointed with red arrows, which are under-segmented by the watershed algorithm. (h) Cluster-separation using a Euclidean distance transform. The under-segmented clusters in (g) are further segmented, as the red arrows pointed out in (g). (i) Morphological filtering on the identified objects. Small artefacts, such as the one indicated by black arrow in (h), are removed.

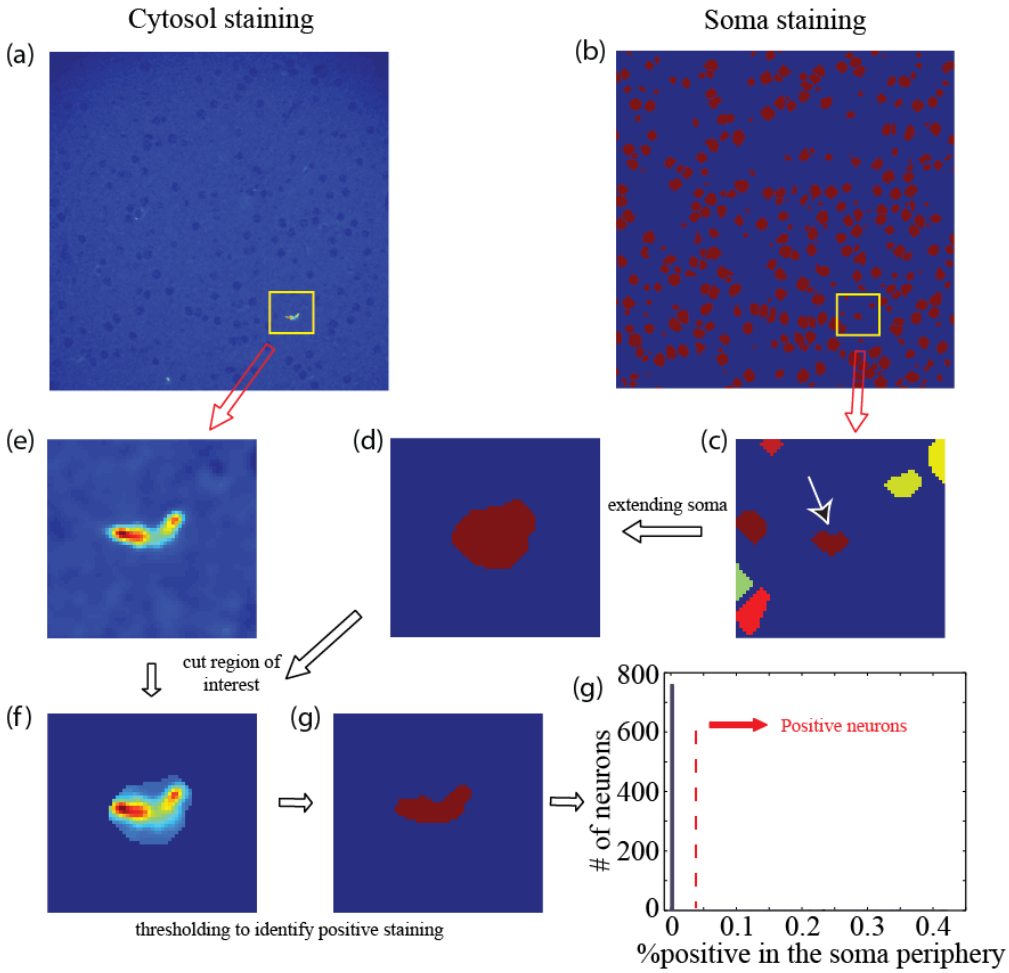

Supplemental Figure 2.

Automatic cell counting for cytosol-staining channels. The example shown is a Somatostatin (SST) staining immunofluorescent image. (a, b) Images from SST-channel and identified cell objects from soma-staining channels, at the same position in the image stack. (c) The cell object under analysis, as indicated by the red arrow, with region of interest marked by yellow rectangle in (a) and (b). (d) The cell object under analysis is enlarged by 2-pixels in all directions; other objects are ignored. (e) Corresponding region in the SST channels. (f) The object in (d) is used as mask image to obtain the region of interest in the SST channel. (g) Positive staining is detected as connected pixels with at least 10% volume of object in (d), whose intensity value is two times the standard deviation higher than average pixel intensity in the local image region as shown in (c). (h) Histogram of percentage of positive staining in the SST channel for all the cell objects identified in (b). Cells with a positive percentage higher than 9% are labelled as SST-positive cells.

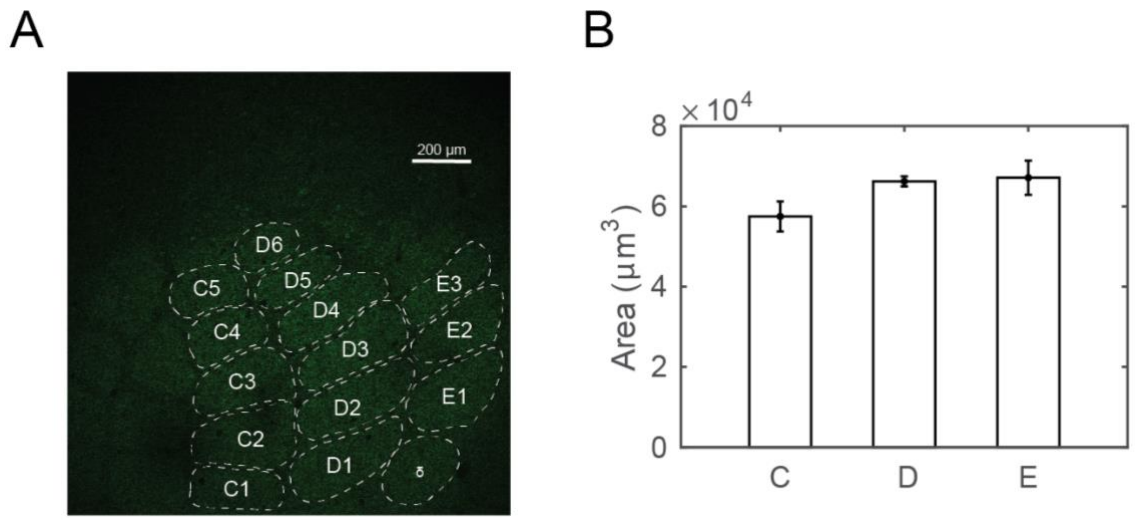

Supplemental Figure 3.

Average volume of a cortical column. (A) A sample image stained with anti-GAD67 antibody overlaid with manually determined barrel borders. (B) Average area of the Layer 4 across barrel columns C, D, and E.

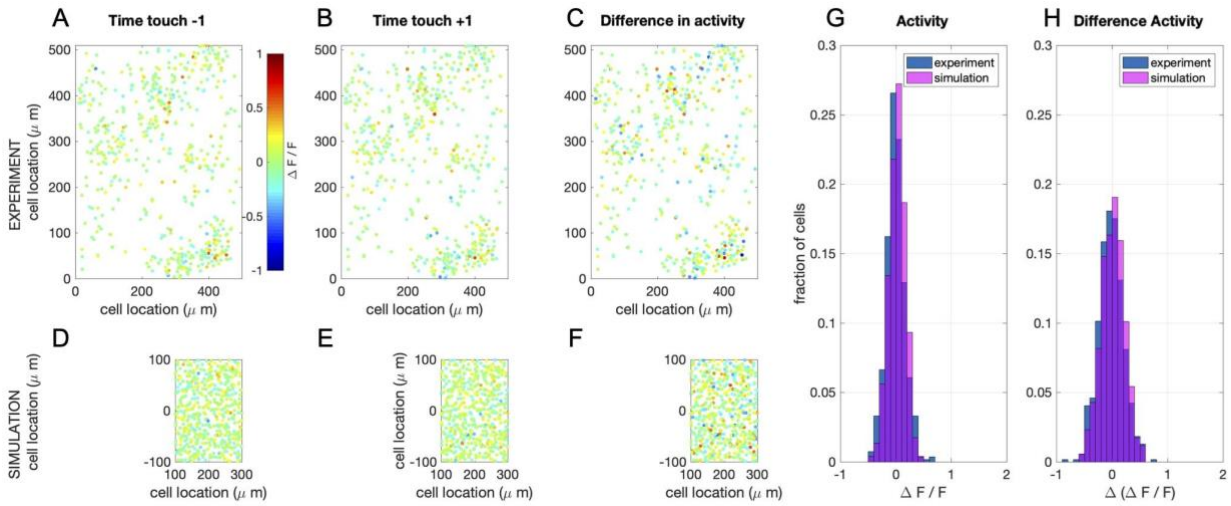

Supplemental Figure 4.

Simulation of calcium imaging experiment in L4 (see main text Figure 9). (A) Recorded network response 1 time frame before touch (sampling frequency: 7 Hz; recorded volume: 8). **(B)** Recorded network response 1 time frame after touch **(C)** Difference in network response between before and after touch. **(D-F)** Same as in A-C, but now for simulations (full simulation: single barrel including L23 and L4 (shown here)). Note that a recorded volume is larger than a single barrel. The frames are scaled accordingly. **(G)** Comparison of the distribution of activity of 1 time frame after touch between the recorded and the simulated network. **(H)** Comparison of the distribution of the difference in activity between 1 time frame before and after touch between the recorded and the simulated network.

2. Supplemental Tables

Citation	Brain regions	Model neurons	Number of neurons in the model	Synaptic plasticity		Comp. platform	Open source toolbox
				Short term	Long term		
Traub et al. 2005	Rat thalamus & cortex	MC conductance	3560	No	No	Cluster	No
Markram et al. 2006	Cortical column	MC conductance	10K	Yes	No	Blue Brain infrastructure, supercomputer	No
Izhikevich & Edelman 2008	Mammalian brainstem, thalamus, cortex	Izhikevich neuron - MC	1M	Yes	STDP	Cluster	No
Ananthanarayanan et al. 2009	Cat visual thalamus and cortex	Izhikevich neuron - Point neuron	>1M	No	STDP	Super computer	No
Zhu et al. 2009	Macaque V1, L4	Leaky integrate and fire	16384	No	No	Unknown	No
Phoka et al. 2012	Rodent barrel cortex L2-4	Izhikevich neuron - MC	3717	No	STDP	NEST	No
Reimann et al. 2013	Rodent neocortical column	MC conductance	hundreds	No	No	NEURON, Blue Brain infrastructure, supercomputer	No
Potjans & Diesmann, 2014	Cortical microcircuit	Leaky integrate-and-fire	80K	No	No	NEST, cluster	Yes (NEST website)
Sharp et al.	Rodent	Leaky	50K	No	No	Cluster	No

2014	barrel cortex	integrate and fire				(SpiNNaker)	
Markram et al. 2015	Rat thalamus and hindlimb S1	MC conductance	31K	Yes	Yes*	Super computer	No
Tomsett et al. 2015	Macaque neocortical network	Reduced MC conductance	>100K	No	No	Matlab, desktop computer	Yes (ModelDB)
Chariker et al. 2016	Macaque V1	Leaky integrate-and-fire	4K	No	No	Unknown	No
Sudhakar et al. 2017	Cerebellar granular layer	MC conductance	800K	No	No	NEURON, cluster	Yes (ModelDB)
Smith et al. 2018a, Schmidt et a. 2018b, Schuecker et al. 2017	Macaque visual cortex, long range connectivity	Leaky integrate and fire	~300K	No	No	NEST, Juqueen supercomputer	Yes (https://inm-6.github.io/multi-area-model/)
Allen Brain Arkhipov et al. 2018, Billeh et al. 2019	Mouse thalamus, L4 visual cortex	Hodgkin-Huxley style conductance and leaky integrate-and-fire	230K	No	No	Cluster (HH) / desktop (IF)	Yes (brain-map.org)
Bernardi et al. 2020	Rodent barrel cortex	Leaky integrate and fire	2600	Yes	No	Unknown	No
Huang et al (Current article)	Rodent thalamus L2-4 barrel cortex	Modified Izhikevich neuron - Point neuron	4200 (depends on number of columns created)	Yes	STDP	Matlab, desktop computer	Yes (on GitHub)

Supplemental Table 1.

Summary of bioinspired cortical network models. MC: Multi compartmental. S1: Primary somatosensory cortex. * The type of long-term synaptic plasticity model is unknown.

	Layer 2/3	Layer 4	Layer 5a	Layer 5b	Layer 6
NeuN+	2410 ± 154	1557 ± 192	709 ± 133	811 ± 68	1226 ± 232
GAD67+	6.5 ± 0.7%	5.5 ± 0.6%	9.5 ± 1.7%	10.2 ± 3.9%	6.8 ± 1.7%
PV+	5.3 ± 1.2%	3.3 ± 0.4%	13.0 ± 5.6%	9.4 ± 3.1%	5.3 ± 0.3%
SST+	1.5 ± 0.5%	1.5 ± 1.1%	3.1 ± 3.4%	1.7 ± 1.8%	1.7 ± 1.0%
CR+	0.9 ± 0.1%	1.2 ± 0.2%	0.8 ± 0.5%	0.4 ± 0.2%	0.6 ± 0.5%

Supplemental Table 2

Distribution of distinct cell populations in a canonical (D-row) barrel cortical column. Values are mean ± std. The estimates are based on 3D reconstructions across five animals, except in Layer 5b (N=3) and Layer 6 (N=2). All values, except NeuN+, are in respect to the NeuN+ cell count within the corresponding layer.

Presyn. neuron	Postsyn. neuron	Ampli-tude (mV)	Rise time (ms)	Decay time (ms)	PPR	Failure rate (%)	CV	Hit rate	Ref **
Thalamic projections into the L4									
Thalamic	Cortical excitatory	0.95 ± 1.10	1.16 ± 0.27	22.5 ± 27.4	0.76 ± 0.07	0.00 ± 0.01[2]	0.23 ± 0.15[2]	0.43[3]	A, B, C
	Cortical fast spiking	1.62 ± 1.26[1]	0.41 ± 0.15	6.74 ± 1.10	0.55 ± 0.12	0.00 ± 0.01[2]	0.22 ± 0.12[2]	0.5[3]	
	Cortical non-fast spiking	0.27 ± 0.19[1]	1.12 ± 0.48	22.5 ± 11.10	0.76 ± 0.07	0.00 ± 0.01[2]	0.72 ± 0.34[2]	0.5[3]	
L4 – L4 connections									
L4 excitatory	L4 excitatory	1.1 ± 1.1	0.88 ± 0.26	12.3 ± 2.2	0.65 ± 0.16	0.11 ± 0.18	0.30 ± 0.19	0.06	A
	L4 fast spiking	2.2 ± 2.2	0.37 ± 0.11	4.9 ± 1.9	0.65 ± 0.16	0.03 ± 0.08	0.27 ± 0.13	0.43	
	L4 low-threshold spiking	0.3 ± 0.5	0.86 ± 0.48	8.9 ± 2.9	1.2 ± 0.3	0.57 ± 0.35	1.04 ± 0.54	0.57	
L4 fast spiking	L4 cells	1.1 ± 0.8	1.5 ± 0.7	24.0 ± 10.8	0.72 ± 0.25	0.03 ± 0.07	0.25 ± 0.11	0.44	
L4 low-threshold spiking	L4 cells	0.48 ± 0.45	2.1 ± 1.0	22.6 ± 13.7	0.99 ± 0.26	0.29 ± 0.26	0.41 ± 0.21	0.35	
L4 – L2/3 connections									
L4 excitatory	L2/3 pyramidal	0.7 ± 0.6	0.8 ± 0.3	12.7 ± 3.5	0.90 ± 0.39	4.9 ± 8.8	0.27 ± 0.13	0.12	D
	PV+ fast-spiking cell	0.96 ± 0.93	0.89 ± 0.31	15.0 ± 8.2	0.99 ± 0.66	20.0 ± 20.0	0.27 ± 0.13*	0.2[4]	E, F
	PV+ bursting cell	1.2 ± 0.2	0.42 ± 0.1	6.3 ± 2.1	0.84 ± 0.17	13.0 ± 19.8	0.5 ± 0.3*		
	Martinotti neuron	Not connected							
	Neurogliaform cell	0.59 ± 0.21	0.85 ± 0.26	13.0 ± 6.2	0.70 ± 0.18	17.0 ± 14.0	0.5 ± 0.3*	0.2[4]	

	CR+ bipolar cell	1.3 ± 0.9	1.1 ± 0.4	14.0 ± 4.1	1.00 ± 0.62	13.0 ± 19.8	0.5 ± 0.3*		
	CR+ multipolar cell	1.4 ± 1.4	0.79 ± 0.50	8.5 ± 3.1	0.92 ± 0.40	13.0 ± 19.8	0.5 ± 0.3*		
	VIP+/CR- cell	1.3 ± 0.9	1.1 ± 0.4	14.0 ± 4.1	1.00 ± 0.62	13.0 ± 19.8	0.5 ± 0.3*		
L4 fast spiking	L2/3 cells	1.1 ± 0.8	1.5 ± 0.7	24.0 ± 10.8	0.72 ± 0.25	0.03 ± 0.07	0.25 ± 0.11	†	A, V
L4 low-threshold spiking	L2/3 cells	Not connected							N/A
L2/3 – L2/3 connections									
L2/3 pyramidal	L2/3 pyramidal	1.0 ± 0.7	0.7 ± 0.2	15.7 ± 4.5	0.61 ± 0.41	3.2 ± 7.8	0.33 ± 0.18	0.10	F, G
	PV+ fast-spiking cell	0.82±0.49	2.32 ± 1.00	16.25 ± 5.78	0.70 ± 0.14	20.0 ± 20.0	0.6 ± 0.1*	0.65	G, V
	PV+ bursting cell	0.38±0.25	2.76 ± 1.05	19.2 ± 2.2	0.51 ± 0.13	13.0 ± 19.8	0.5 ± 0.3*	0.18	H
	Martinotti neuron	0.25±0.2	2.76 ± 1.05	19.2 ± 2.2	1.91 ± 0.82	50 ± 20	1.04 ± 0.54	0.29	I, J, P
	Neurogliaform cell	0.39±0.33	2.6 ± 0.5	17.9 ± 4.0	0.83 ± 0.14	20 ± 10	0.6 ± 0.1*	0.29	G, S
	CR+ bipolar cell	1.35±0.62	0.64 ± 0.27	26.0 ± 8.1	0.83 ± 0.14	28 ± 22	0.39 ± 0.07	0.18	K, N
	CR+ multipolar cell	1.36±0.78	1.26 ± 0.53	9.5 ± 3.9	1.6 ± 0.7	50 ± 20	0.6 ± 0.1*	0.20	M, N
	VIP+/CR- cell	1.35±0.62	0.64 ± 0.27	26.0 ± 8.1	0.83 ± 0.14	28 ± 22	0.39 ± 0.07	0.46	M, I
PV+ fast-spiking cell	L2/3 pyramidal	0.52±0.45	3.5 ± 1.4	43.1 ± 10.2	0.70 ± 0.15	5.1 ± 8.7[5]	0.46 ± 0.17[5]	0.60	G, S
	PV+ fast spiking cell	0.56±0.43	1.8 ± 0.6	15.8 ± 6.0	0.70 ± 0.15	5.1 ± 8.7[5]	0.46 ± 0.17[5]	0.55	G, S
	others	Not connected							U
PV+ bursting	L2/3 pyramidal	1.21 ± 1.18	2.1 ± 1.0	22.6 ± 13.7	1.27 ± 0.60	8.9 ± 11.8[5]	0.53 ± 0.23[5]	0.41	H, O

cell	PV+ fast-spiking cell	0.77 ± 0.62	2.1 ± 1.0	22.6 ± 13.7	0.86 ± 0.20	5.1 ± 8.7[5]	0.46 ± 0.17[5]	0.26	
	others	1.06 ± 0.83	2.1 ± 1.0	22.6 ± 13.7	1.53 ± 0.63	8.9 ± 11.8[5]	0.53 ± 0.23[5]	0.41	
Martinotti neuron	Martinotti neuron	Not connected							P, T, U
	others	0.29 ± 0.22	3.5 ± 1.1	13.7 ± 9.9	1.80 ± 0.50	26.8 ± 26.3[5]	0.91 ± 0.56[5]	0.71	
Neurogliaform cell	others	0.58 ± 0.1	53.2 ± 10.8	100 ± 19	0.51 ± 0.13	5.1 ± 8.7[5]	0.46 ± 0.17[5]	0.44	Q, O, R
CR+ bipolar cell	L2/3 pyramidal	0.49 ± 0.49[6]	5.4 ± 2.2[6]	56.2 ± 24.1[6]	1.40 ± 0.50	26.8 ± 26.3[5]	0.91 ± 0.56[5]	0.11	L, O, St
	PV+ fast-spiking cell	0.37 ± 0.33[6]	3.1 ± 2.0[6]	20.0 ± 12.1[6]	1.10 ± 0.20	26.8 ± 26.3[5]	0.91 ± 0.56[5]	0.30	
	CR+ bipolar cell	0.49±0.56[6]	4.9 ± 5.4[6]	33.3 ± 12.0[6]	1.42 ± 0.20	26.8 ± 26.3[5]	0.91 ± 0.56[5]	0.32	
	CR+ multipolar cell	0.49±0.56[6]	4.9 ± 5.4[6]	33.3 ± 12.0[6]	1.33 ± 0.30	26.8 ± 26.3[5]	0.91 ± 0.56[5]	0.76	
	others	0.49±0.56[6]	4.9 ± 5.4[6]	33.3 ± 12.0[6]	1.80 ± 0.30	26.8 ± 26.3[5]	0.91 ± 0.56[5]	0.30	
CR+ multipolar cell	L2/3 pyramidal	0.49±0.49[6]	5.4 ± 2.2[6]	56.2 ± 24.1[6]	0.7 ± 0.3	5.1 ± 8.7[5]	0.46 ± 0.17[5]	0.14	L, O, S
	PV+ fast-spiking cell	0.37±0.33[6]	3.1 ± 2.0[6]	20.0 ± 12.1[6]	1.4 ± 0.4	26.8 ± 26.3[5]	0.91 ± 0.56[5]	0.18	
	CR+ bipolar cell	0.49±0.56[6]	4.9 ± 5.4[6]	33.3 ± 12.0[6]	0.98 ± 0.2	8.9 ± 11.8[5]	0.53 ± 0.23[5]	0.41	
	CR+ multipolar cell	0.49±0.56[6]	4.9 ± 5.4[6]	33.3 ± 12.0[6]	0.74 ± 0.30	5.1 ± 8.7[5]	0.46 ± 0.17[5]	0.10	
	others	0.49±0.56[6]	4.9 ± 5.4[6]	33.3 ± 12.0[6]	1.1 ± 0.4	8.9 ± 11.8[5]	0.53 ± 0.23[5]	0.50	
VIP+/CR- cell	L2/3 pyramidal	0.49±0.49[6]	5.4 ± 2.2[6]	56.2 ± 24.1[6]	1.0 ± 0.3	8.9 ± 11.8[5]	0.53 ± 0.23[5]	0.46[6]	L, O, S
	PV+ fast-spiking cell	0.37±0.33[6]	3.1 ± 2.0[6]	20.0 ± 12.1[6]	1.0 ± 0.3	8.9 ± 11.8[5]	0.53 ± 0.23[5]	0.38[6]	
	others	0.49±0.56[6]	4.9 ± 5.4[6]	33.3 ± 12.0[6]	1.0 ± 0.3	8.9 ± 11.8[5]	0.53 ± 0.23[5]	0.38[6]	

Supplemental Table 3

Features of neural connectivity in the somatosensory (barrel) cortical column. Pconn, connection probability; PPR, paired pulse ratio. Values are mean ± std.

Notes:

† Same parameters are used as in L4-L4 connections, but extended into L2/3. * Values reflect L4-L4 connections. ** References: (A) Beierlein et al 2003; (B) Gil et al 1999; (C) Bruno & Sakmann 2006; (D) Feldmeyer et al 2002; (E) Helmstaedter et al 2008; (F) Sun et al 2006; (F) Feldmeyer et al 2006; (G) Holmgren et al 2003; (H) Blatow et al 2003; (I) Ali 2003; (J) Kapfer et al 2007; (K) Reyes et al 1998; (L) Rozov et al 2001; (M) Porter et al 1998; (N) Caputi et al 2009; (O) Gupta et al 2000; (P) Fino & Yuste 2011; (Q) Wozny & Williams 2011; (R) Tamas et al 2003; (S) Avermann et al 2012; (T) Packer & Yuste 2011; (U) Pfeffer et al 2013; (V) Koelbl et al 2015. [1] Values are taken from A, but scaled according to C.[2] Values are calculated from L4-L4 connections measured in A, based on the difference between L4-L4 synapses and thalamic-L4 synapses reported in B. [3] Values are for thalamus-L4 connection probability. [4] Values are taken from E, as average connection probability between L4 excitatory neurons and L2/3 interneurons.[5] Values are taken from O, based on inhibitory synapse classification. [6] Values are taken from S, as average values for NFS (non-fast-spiking) interneurons.

	a	b	c	d
L4 neurons				
Excitatory	0.020 ± 0.006	0.225 ± 0.014	-58.0 ± 2.9	9.0 ± 1.7
FS interneuron	0.100 ± 0.012	0.203 ± 0.015	-69.7 ± 3.0	10.6 ± 1.7
Non-FS interneuron	0.021 ± 0.006	0.255 ± 0.028	-59.9 ± 4.3	8.9 ± 1.1
L2/3 neurons				
Excitatory	0.020 ± 0.006	0.225 ± 0.014	-62.0 ± 4.4	11.0 ± 1.7
PV+ FS	0.100 ± 0.011	0.213 ± 0.015	-69.7 ± 3.0	12.6 ± 1.8
PV+ bursting	0.021 ± 0.006	0.240 ± 0.029	-54.7 ± 2.7	6.9 ± 1.2
Martinotti	0.022 ± 0.006	0.225 ± 0.014	-59.8 ± 4.5	8.3 ± 2.1
Neurogliaform	0.021 ± 0.006	0.267 ± 0.015	-85.7 ± 2.7	15.9 ± 1.2
CR+ bipolar	0.020 ± 0.006	0.260 ± 0.014	-55.5 ± 3.9	8.2 ± 1.5
CR+ multipolar	0.024 ± 0.009	0.200 ± 0.012	-62.1 ± 2.8	11.5 ± 1.6
VIP+/CR- cell	0.021 ± 0.006	0.230 ± 0.015	-57.2 ± 4.2	8.1 ± 1.6

Supplemental Table 4

Table 3.2. Model parameters for different types of neurons in the network. All values are mean ± std; parameters are normally distributed. FS: Fast-spiking, PV+: Parvalbumin expressing neurons, CR+: Calretinin expressing neurons, VIP+/CR-: Vasopressin expressing Calretinin negative neurons.

Antibody	Number of image stacks	Average relative difference (%)	Average absolute difference (%)
Anti-NeuN	13	1.24 ± 2.49	2.32 ± 1.42
Anti-Parvalbumin (PV)	7	-0.55 ± 3.49	2.64 ± 2.09
Anti-Calretinin (CR)	7	-0.47 ± 3.24	2.48 ± 1.91
Anti-Somatostatin (SST)	6	1.19 ± 3.52	2.90 ± 2.01
Anti-GAD67	7	1.68 ± 6.76	5.56 ± 3.60

Supplemental Table 5

Comparison of automated counting and manual counting results for different antibody staining. Across all different antibody staining the average relative difference is below 2% when the automated counting results were compared with average results obtained by independent human observers.